· LA-UR -86-3043 CONF-860815--2

Los Alamos National Laboratory is operated by the University of California for the United States Department of Energy under contract W-7405-ENG-36

LA-UR--86-3043

DE87 000135

TITLE: OPTIMIZATION OF A HE-JET ACTIVITY TRANSPORT SYSTEM TO USE AT LAMPF

AUTHOR(S): W. L. Talbert, INC-11
M. E. Bunker, INC-5
J. W. Starner, INC-5

SUBMITTED TO: 11th Int'l Conf. on Electromagnetic Isotope Separators and Techniques Related to their Applications, Los Alamos, NM August 18-22, 1986

DISCLAIMER

Los Alamos Los Alamos National Laboratory
Los Alamos, New Mexico 87545

OPTIMIZATION OF A HE-JET ACTIVITY TRANSPORT SYSTEM TO USE AT LAMPF*

W. L. TALBERT, JR., M. E. BUNKER and J. W. STARNER

Los Alamos National Laboratory, Los Alamos, New Mexico 87545, USA

As part of an assessment of the feasibility for a He-jet coupled on-line mass separator at LAMPF, we have studied performance characteristics of a gas activity transport system under conditions simulating those expected on the main LAMPF beam line. In experiments utilizing a side beam at LAMPF, we have measured absolute transport efficiencies, transit times, aerosol properties, and dependences on beam intensity. Further experiments with a He-jet system at the Omega West Reactor have indicated an optimum configuration of a target chamber to be placed in the LAMPF main beam. The results of these studies suggest that a He-jet activity transport system should work well at LAMPF in the 800-MeV, 1-mA proton beam that is spread over ~40 cm^2 near the beam stop.

1. Introduction

The intense proton beam available at LAMPF has long been considered a unique means of producing copious quantities of nuclei far from the line of beta stability. Since 1970, various proposals for an on-line isotope separator (ISOL) at LAMPF have been prepared, but all were either considered too costly or were subject to questions about our estimated yields of nuclei far from stability. For the past four years we have been investigating the feasibility of using a He-jet coupled ISOL system at LAMPF. These studies initially considered the suitability of He-jet activity transport under conditions expected in the main beam of LAMPF near the beam stop.

We were attracted to the He-jet approach by several favorable factors. The cost of such an approach would be modest because no large quantities of

* Work supported by the U. S. Department of Energy.

additional shielding would be required. At the time we initiated these studies, the technique of coupling a He-jet transport system to a mass separator seemed to be well on the way to solution in view of successful installations at several laboratories throughout the world [1-8]; indeed there are recent experiments that have demonstrated improved throughput efficiencies for a number of nonvolatile species [9-11]. In addition, there were available some excellent studies [12-14] of He-jet transport that proved to be invaluable.

A strong motivation exists to make systematic studies of nuclear properties, excitations, and decay modes over as large a range of element number and mass number as possible. The He-jet technique offers unique capabilities in this endeavor because essentially all elements produced in nuclear reactions involving recoiling products (virtually all reactions possible with energetic protons have recoiling products) can be transported to a mass separator and introduced into the ion source, including the nonvolatile elements. Hence, a number of elements not available at other ISOL facilities are uniquely available with a He-jet system.

Other factors favorable to a He-jet system at LAMPF include: both fission and spallation products can be studied; since the target is placed in the main beam line, operation of the proposed ISOL system is parasitic to the operation of LAMPF, assuring high availability; the production rates even for the required thin targets are roughly equivalent to those obtained at thick-target ISOL facilities due to the very large proton beam intensity; and the use of thin targets avoids limitations imposed by target diffusion and desorption processes present for thick systems.

Feasibility studies were thus conceived to assure that a He-jet system could be successfully operated at LAMPF, and that the system parameters could

be optimized prior to installation (in recognition that any changes made in a target chamber located in the main LAMPF beam line would undoubtedly be time-consuming and expensive).

2. Experimental program

The problems addressed in our feasibility study were: 1) Will the He-jet technique work at the beam intensities that exist at LAMPF?; 2) what transport efficiencies can be expected for both fission and spallation products?; 3) what is the time dependence of the activity transported?; 4) what is the optimum target chamber configuration?; and 5) what aerosols and/or aerosol conditions are optimum?

Two sets of experiments were performed at LAMPF in response to these issues. Both sets were performed using the LAMPF H^- beam, which was more accessible for feasibility studies than the main LAMPF beam. In these experiments, we measured the absolute values of transport efficiencies for a wide range of elements, as well as the dependence of transport efficiencies on beam current density, aerosol conditions, and capillary flow.

The absolute transport efficiencies were measured by comparing counting rates for known activities in samples collected after transport with the same activities in samples collected by catching direct recoils from the targets on beryllium catcher foils. Thus, the measured efficiencies reflect not only the transport efficiency through the capillary, but also the efficiency of activity attachment to aerosols and subsequent entrainment of aerosols into the helium flow through the capillary.

The main LAMPF beam near the beam stop is expected to have an effective diameter of about 7 cm and a maximum current density of about 35 $\mu A/cm^2$. We

employed a target chamber with 7.6-cm diameter targets so that the target stopping volume would be reasonably realistic (about 650 cm^3-bar), even though the H^- beam at LAMPF had a thin, horizontal profile of approximately 20 mm^2 at the target position.

Because of the difficulty of making systematic studies to derive optimum operational conditions through use of the infrequently available H^- beam at LAMPF, we installed a He-jet target chamber in a neutron beam port at the Los Alamos Omega West Reactor (OWR) to continue these studies. A target chamber was constructed to investigate the effects on transport times and target volume sweep rates of using multiple capillary outlets and helium inlets. The neutron beam, of flux 4 x 10^8 n/cm^2-s, was 7.6 cm in diameter to simulate the main LAMPF beam profile, and it was controlled by a fast-acting cadmium shutter with on-off or off-on action within 5 ms to allow measurements of transport times and target volume sweep rates. Also, we evaluated the three candidate aerosol materials NaCl, KCl and $PbCl_2$ to determine which would provide the highest transport efficiency.

In the above experiments, we generated the aerosols by using a ceramic boat loaded with aerosol salt, which was inserted into a temperature-controlled tube furnace. The helium stream was passed over the heated boat and into the target chamber through a 6.35-mm diameter line of length 20 m that served as an aerosol size filter. From the target chamber, a 22-m long capillary led into a collection chamber that was evacuated by a high-capacity Roots pumping system. The capillary end was positioned 3 to 5 mm from a collection disc or movable tape, where the aerosols and attached activities were deposited in a spot about 1.5 mm in diameter.

Additional measurements were made of aerosol properties using an

electrical aerosol analyzer (EAA) [15] in which the aerosol and temperature variations simulated those used in the LAMPF and OWR experiments. The simulations were verified by collecting aerosol samples during the LAMPF experiments through a diffusion battery [16] and comparing the measured aerosol size distributions and number densities with the off-line simulated values. We also collected samples of aerosols for examination with a transmission electron microscope.

3. Results

3.1 LAMPF Results

Absolute transport efficiencies were measured for a capillary length of 22 m, the projected length to connect the target chamber in the main LAMPF beam to an ISOL system. Using $PbCl_2$ aerosols, we found these efficiencies averaged about 60% for the more refractory-element activities having half-lives from 5 to 15 minutes. There were essentially no differences between fission-product and spallation-product efficiencies despite the fact that spallation products recoil with considerably shorter range than fission products. Virtually all expected nonvolatile elements were seen, including the rare-earth elements from fission of ^{238}U and spallation of tantalum, and the transition metals from fission of ^{238}U and spallation of rhodium.

A moving tape collector was used at the collection chamber to provide the capability of observing short-lived activities in the half-life range of 1 to 5 s. The observed counting rates of the $^{238}U(p,f)$ products were very high, and in the resulting spectra, many of the gamma-ray peaks could not be identified from previously reported studies. At high target chamber pressures (up to 600 kPa), the short-lived activity levels were much higher than those

observed at 200 kPa, a result of the higher capillary flow rates and faster transport at higher pressures. The highest target chamber pressures used (500 and 600 kPa) resulted in capillary flow for which the Reynolds number approached 5000, considerably exceeding conventional laminar flow design limits of about 2200. However, the rate of activity transport continued to increase smoothly when these pressures were used. We conclude that any turbulence resulting from the high flow did little to disturb the transport of the heavy aerosols, in accordance with ref. [17].

Transit time measurements were performed for various conditions, the shortest time being 230 ms for a target chamber pressure of 500 kPa. The activity coming from the capillary was collected on a moving tape and transported to a well-collimated detector viewing a small region of the tape. The time of tape transport was considered in the measurement. These results are convincing that activities as short as 300-ms half-life could be readily studied with a He-jet transport system at LAMPF.

We varied the proton beam current over a range of 1.5 μA to 6.1 μA and observed no variation in the transport efficiency; i.e., the activity transported rose linearly with the total beam current. Post-experiment scans of the beam-induced activities in the ^{238}U target foils indicated that, at the highest current, a beam current density of 45 $\mu A/cm^2$ had been achieved. The highest expected beam current density at the LAMPF beam-stop area is well below this number; hence, we conclude that the He-jet transport system should function satisfactorily in the intense LAMPF beam, which has been a major concern.

The temperature dependence of the amount of transported activity verified directly that the activity attaches to the aerosols according to total surface

area, as shown in fig. 1, where the transported activity as a function of temperature is compared to simulation measurements of aerosol area and number density using the EAA. The aerosol used was $PbCl_2$. This result had been indicated in other, unrelated studies [18] for aerosols in the size range employed (mean radius of about 0.05 μm). Aerosol samples were collected for electron microscopy, and aerosol size distribution measurements were made on activity-loaded aerosols. The electron microscope pictures of the $PbCl_2$ aerosols revealed that the aerosol particles resemble chains of smaller nucleations - conglomerations having a high ratio of surface area to mass, for which a representative view is shown in fig. 2. The KCl and NaCl aerosols, shown in figs. 3 and 4, have a contrasting, nearly spherical shape.

3.2 OWR Results

In experiments at OWR, we utilized a cylindrical target chamber with 5 possible exit capillaries and three possible inlet lines, shown schematically in fig. 5, to determine empirically the best configuration for efficient and fast activity transport. For this target chamber concept, the use of two inlet lines spaced 90° apart gave superior volume sweep rate and transport efficiency compared to any other combination, and multiple, manifolded capillaries helped only slightly compared to just one (central) outlet. Thus, the simplest high-efficiency design for transporting short-lived activities is a single outlet capillary with two inlets at ± 135° relative to the outlet.

Experiments with various flow rates and capillary diameters showed that activity was swept out from the target-chamber volume more rapidly with a capillary of 2.4-mm diameter than with a 1.6-mm diameter capillary under similar flow conditions, as seen in fig. 6. The transit times as a function of

flow rate appear to follow reasonably well the theoretical predictions [12] shown in fig. 7 for the 2.4-mm diameter capillary.

The aerosol experiments showed a clear advantage for the use of $PbCl_2$ at a furnace temperature of about 475°C. Aerosols of NaCl and KCl, also at furnace temperatures about 25°C below their respective melting points (which provided the maximum transport for these aerosols), provided only about 80% of the activity obtained with $PbCl_2$, as seen in fig. 8. This may be due to the high ratio of surface area to the mass of individual $PbCl_2$ aerosol particles. The use of $PbCl_2$ in conjunction with an ion source may also offer the advantage of greater volatility within the ion source and thus faster release of the attached transported activities.

The final configuration for the LAMPF target chamber will include two inlets and a single outlet, and the chamber will be operated at a pressure of 300 kPa for optimum timing, constrained by reasonable helium consumption (see fig. 7).

4. Conclusions and future work

The experiments carried out at LAMPF and OWR have indicated that great promise for scientific study of nuclei far from stability exists for a He-jet activity transport system with the target in the beam stop area of LAMPF. The He-jet technique has been shown to work at LAMPF beam intensities, with transport efficiencies of about 60% for transport over a capillary length of 22 m, and with transit times of about 250 ms. The optimum aerosol for transport was found to be $PbCl_2$, but both KCl and NaCl will yield adequate transport efficiencies if $PbCl_2$ proves not to be suitable for coupling the transport system to an ion source. We are very encouraged about the ease with which the He-jet

transport system operates, and with the reproducibility of results between the conditions at LAMPF and at the OWR.

One remaining concern with the proposed ISOL system is whether adequate efficiency can be attained for coupling a He-jet to an ISOL ion source. We have constructed a test stand at the OWR to carry out coupling studies similar to those of ref. 1. A scaled version of a monocusp ion source [19] has been constructed as a first candidate for coupling efficiency measurements. As these studies progress, we may also test the high-temperature ion source presently in use at the Idaho National Engineering Laboratory (INEL) [11].

We are indebted to S. C. Soderholm and H.-H. Hsu of Los Alamos for assistance in aerosol measurements and in the LAMPF experiments. V. J. Novick and R. J. Gehrke of INEL and R. F. Petry of the University of Oklahoma provided welcome assistance in the LAMPF experiments. C. W. Reich and R. C. Greenwood of INEL have been supportive of the concept of an ISOL at LAMPF and first suggested that we consider evaluating the feasibility of using the He-jet technique as a new approach to our proposal. M. E. Schaffner assisted us in the evaluation of the flow characteristics of the capillary while a summer student at Los Alamos.

References

[1] R. A. Anderl, V. J. Novick and R. C. Greenwood, Nucl. Instr. and Meth. 186 (1981) 153.

[2] J. Ärje, J. Äystö, J. Handanen, K. Valli and A. Hautojarvi, Nucl. Instr. and Meth. 186 (1981) 149.

[3] A. K. Mazumdar, H. Wagner, W. Walcher, M. Brügger and N. Trautmann, Nucl. Instr. and Meth. 186 (1981) 131.

[4] J. P. Zirnheld, L. Schutz and F. K. Wohn, Nucl. Instr. and Meth. 158 (1979) 409.

[5] K. Okano, Y. Kawase, K. Kawade, H. Yamamoto, M. Hanada, T. Katoh and I. Fujiwara, Nucl. Instr. and Meth. 186 (1981) 115.

[6] D. M. Moltz, J. Äystö, M. D. Cable, R. F. Perry, P. E. Haustein, J. M. Wouters and J. Cerny, Nucl. Instr. and Meth. 186 (1981) 141.

[7] H. Schmeing, V. Koslowsky, M. Wightman, J. C. Hardy, J. A. MacDonald, T. Faestermann, H. R. Andrews, J. S. Geiger and R. L. Graham, Nucl. Instr. and Meth. 139 (1976) 335.

[8] D. M. Moltz, Nucl. Instr. and Meth. 186 (1981) 135.

[9] M. Brügger, N. Hildebrand, T. Karlewski, N. Trautmann, A. K. Mazumdar and G. Herrmann, Nucl. Instr. and Meth. A234 (1985) 218.

[10] Y. Kawase, K. Okano and Y. Funakoshi, Nucl. Instr. and Meth. A241 (1985) 305.

[11] R. A. Anderl, J. D. Cole and R. C. Greenwood, these proceedings.

[12] H. Dautet, S. C. Gujrathi, W. J. Wiesenhahn, J. M. D'Auria and B. D. Pate, Nucl. Instr. and Meth. 107 (1973) 49.

[13] W. J. Wiesenhahn, J. M. D'Auria, H. Dautet and B. D. Pate, Can. J. Phys. 51 (1973) 2347.

[14] C. Weiffenbach, S. C. Gujrathi, J. K. P. Lee and A. Houdayer, Nucl. Instr. and Meth. 125 (1975) 245.

[15] Model 3030 Electrical Aerosol Size Analyzer, Thermo Systems Inc., St. Paul, MN.

[16] Model 3040 Diffusion Battery, Thermo Systems Inc. St. Paul, MN.

[17] H. Wollnik, Nucl. Instr. and Meth. 139 (1976) 311.

[18] O. G. Raabe, Health Phys. 14 (1968) 397.

[19] J. P. Brainard and J. B. O'Hagen, Rev. Sci. Instr. 54 (1983) 1497.

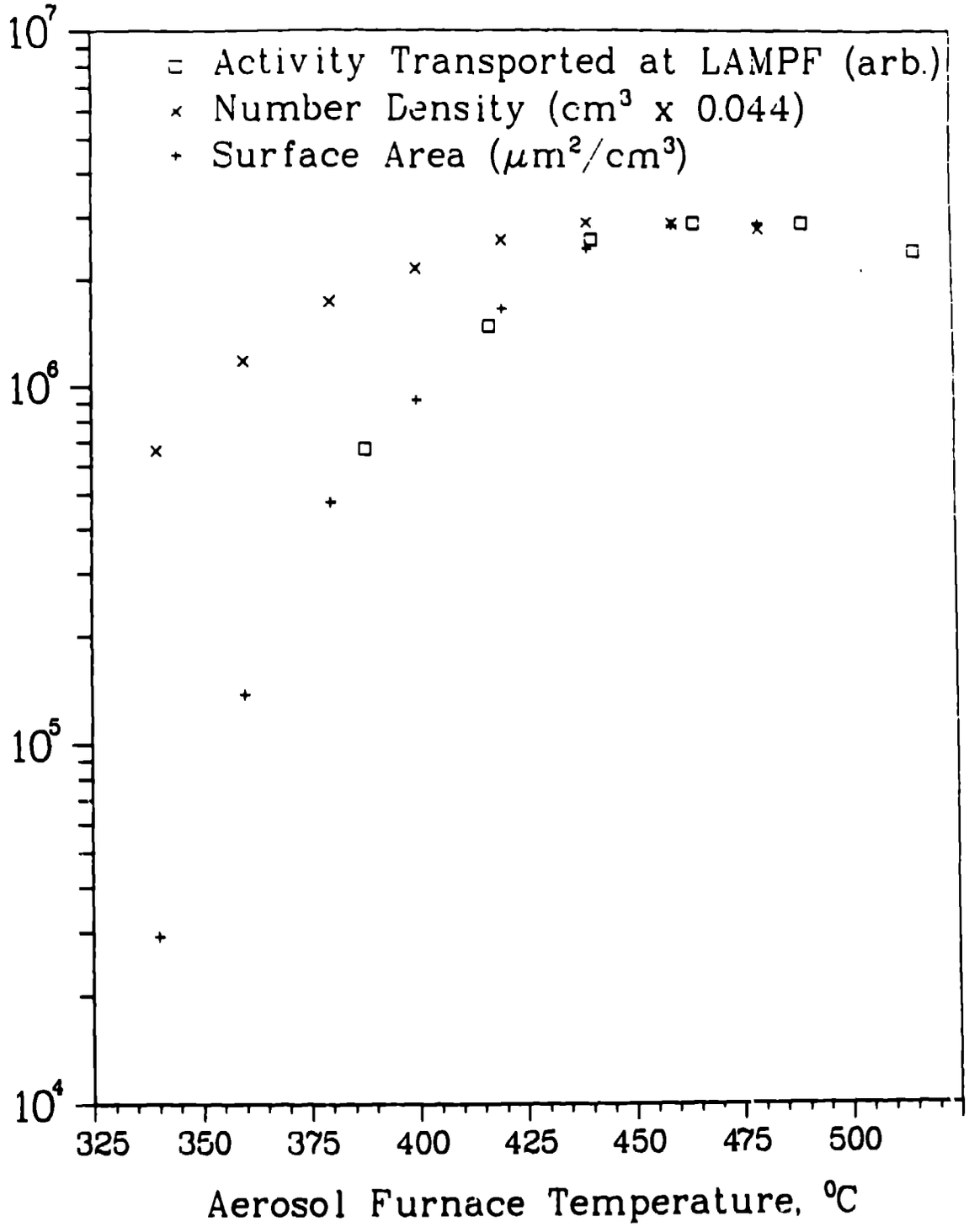

Fig. 1. Dependence of activity transported and aerosol properties ($PbCl_2$) on aerosol furnace temperature.

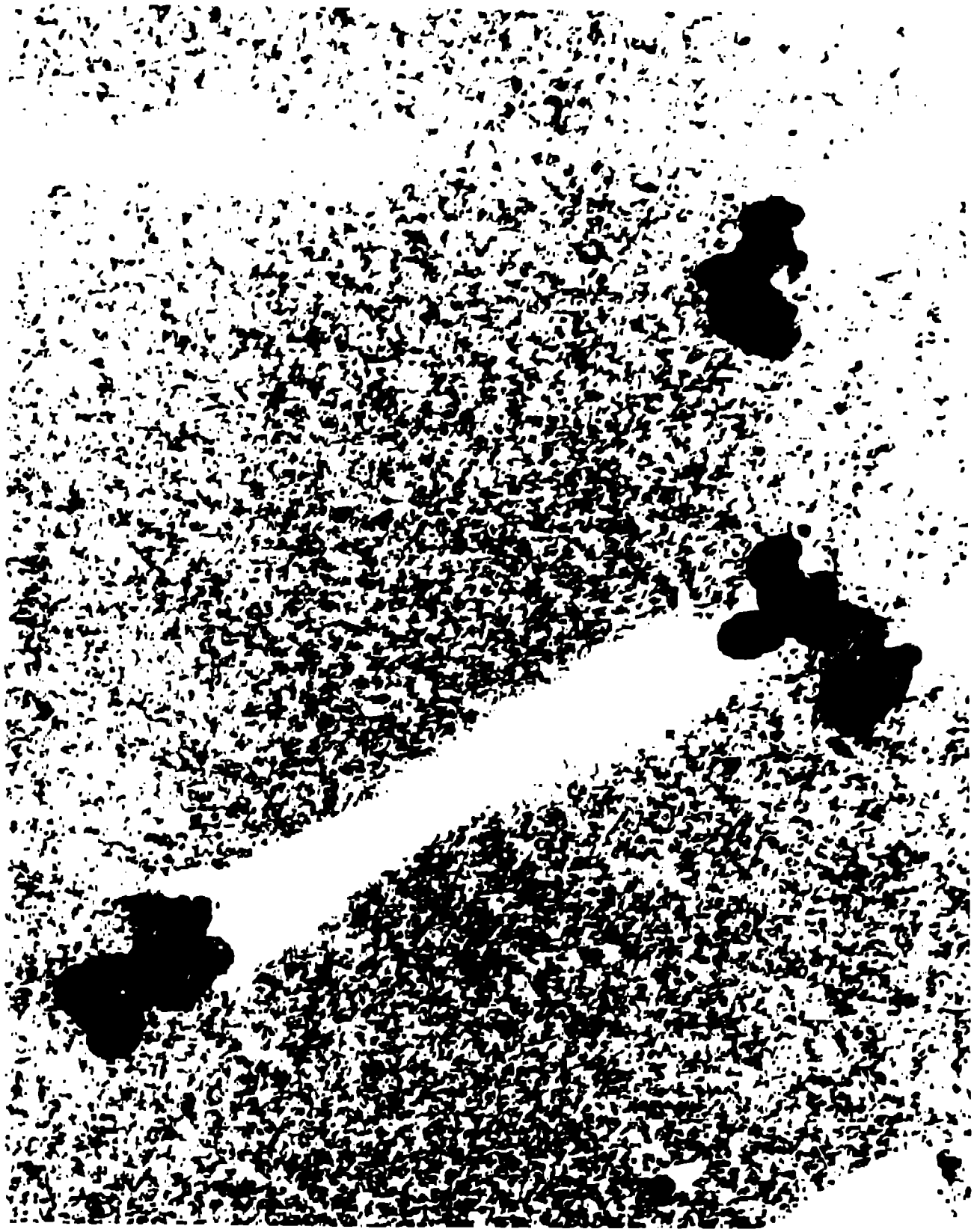

Fig. 2. Electron microscope image of $PbCl_2$ aerosols. The light-colored shadow extending from left to right indicates the height of the aerosol particle above the plane (the shadow was cast at an angle of 30° to the plane). The total view is 1.12 μm wide.

Fig. 3. Electron microscope image of KCl aerosols. Same magnification and shadow angle as for fig. 1.

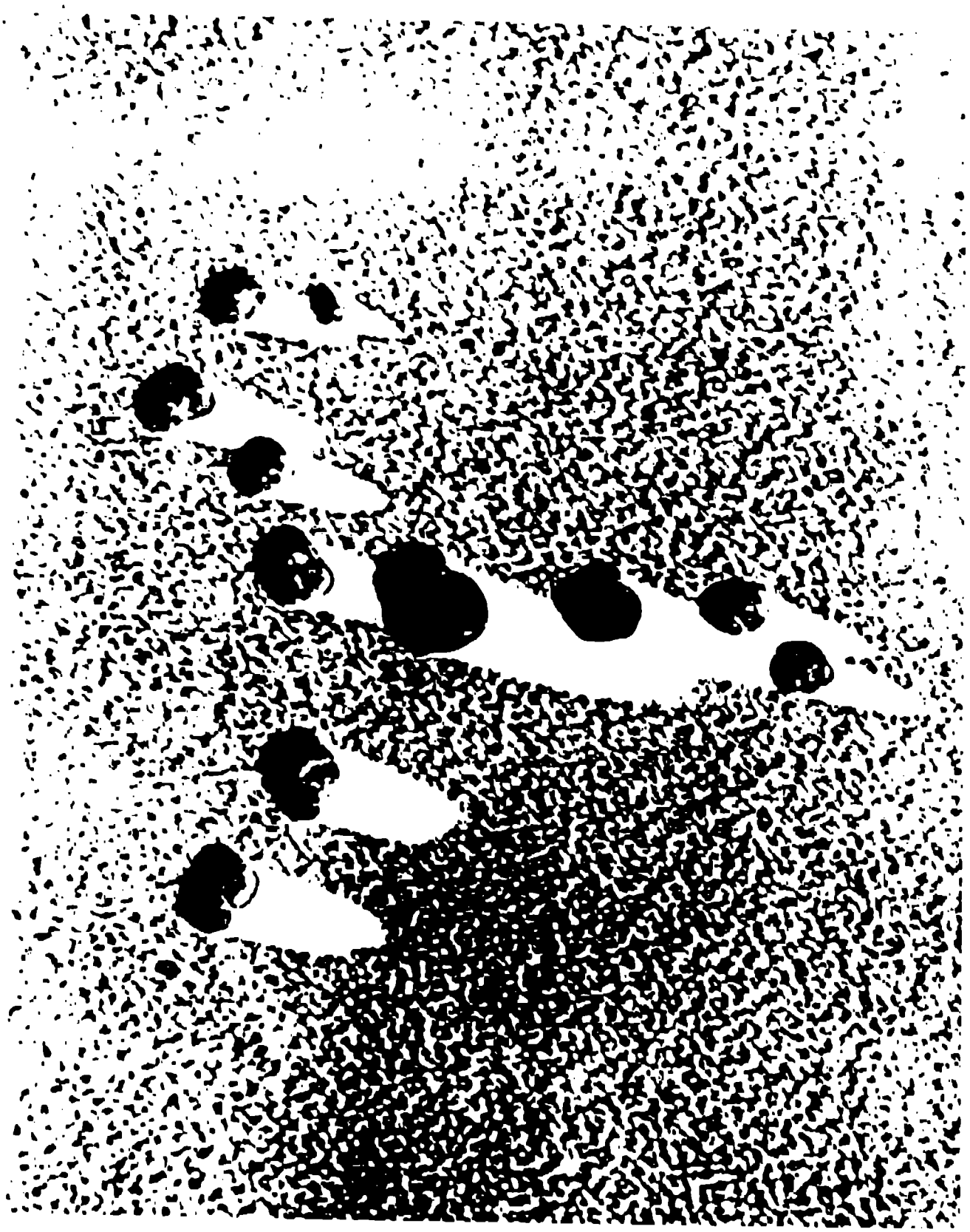

Fig. 4. Electron microscope image of NaCl aerosols. Same magnification and shadow angle as for fig. 1.

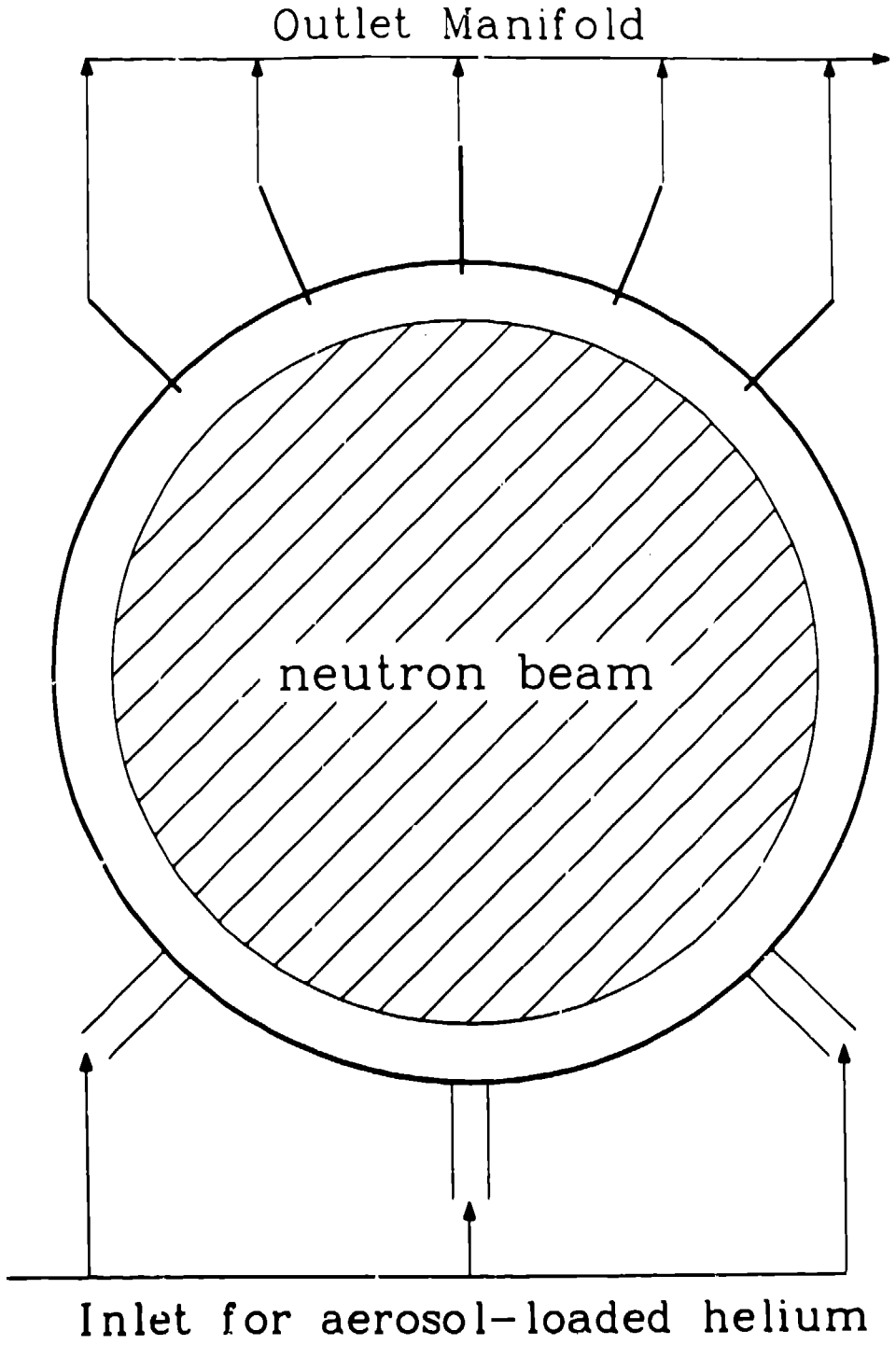

Fig. 5. Schematic diagram of the target chamber used in the OWR experiments.

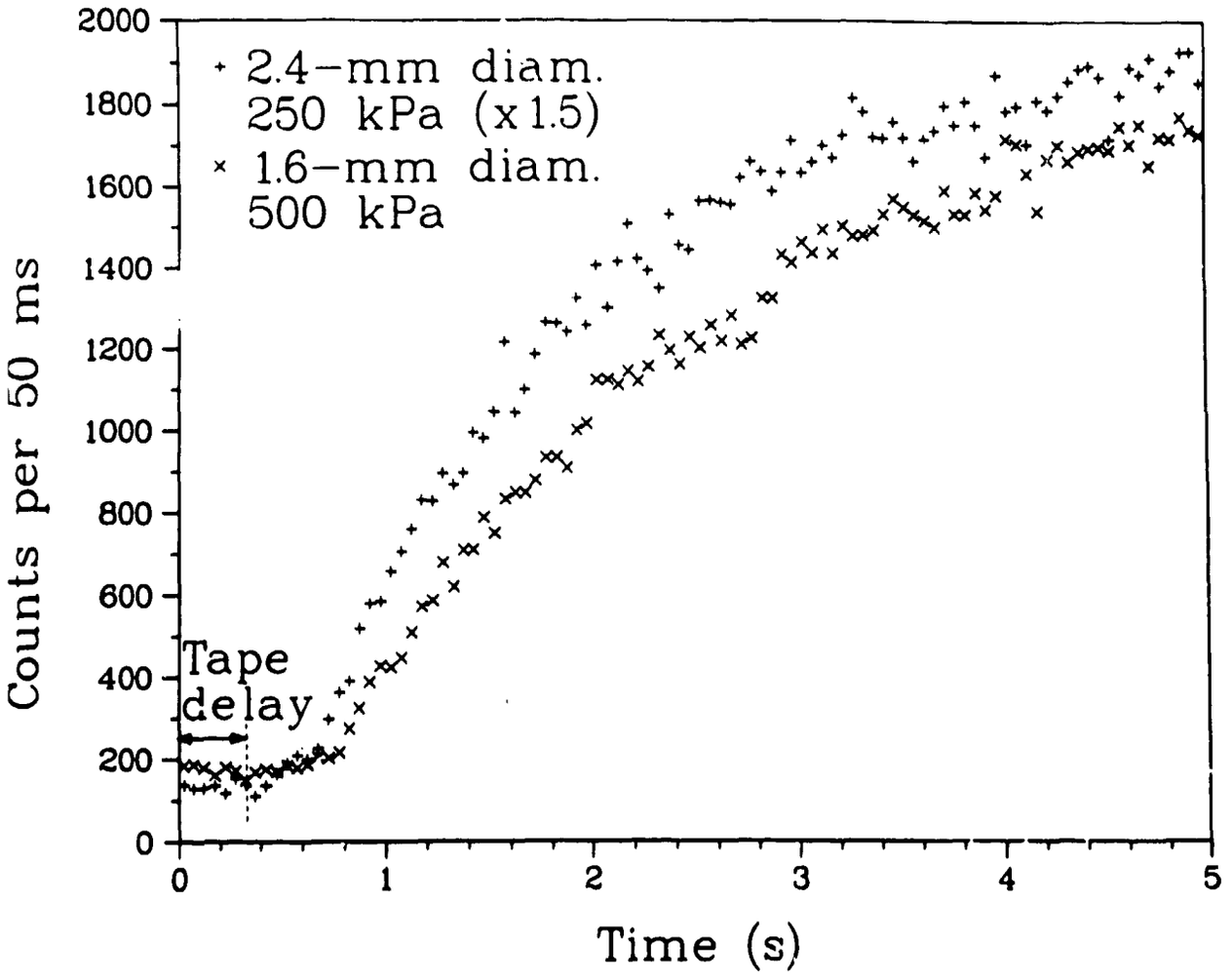

Fig. 6. Activity multiscale after opening the neutron shutter for 1.6-mm and 2.4-mm capillaries. The 2.4-mm data scaling factor of 1.5 for a full-stopping-volume target-chamber thickness was confirmed in a later experiment.

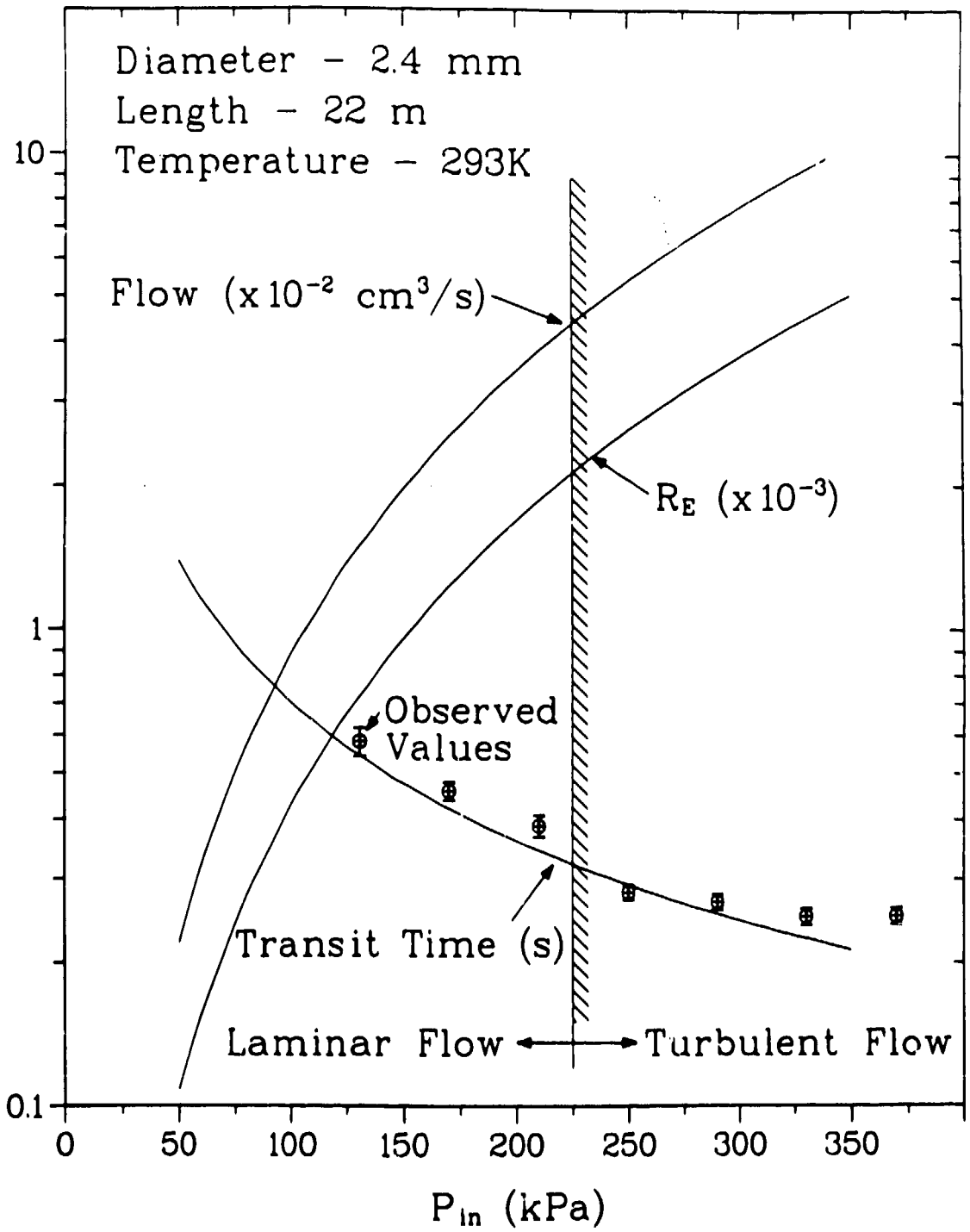

Fig. 7. Theoretical flow quantities for a 2.4-mm diameter capillary as a function of target chamber pressure, showing the measured transit times through the capillary.

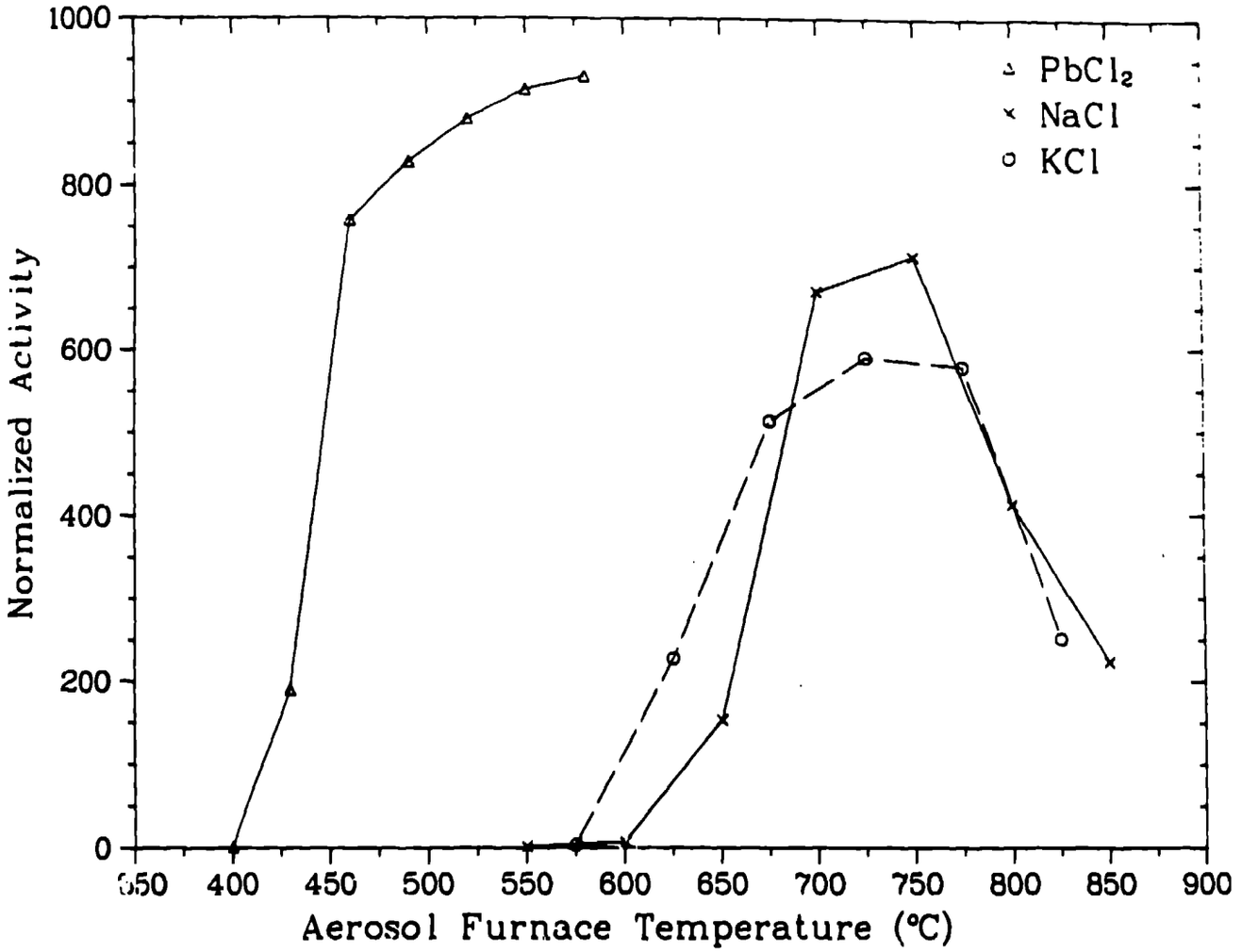

Fig. 8. Relative aerosol transport efficiencies as a function of aerosol furnace temperature for a 22-m long, 2.4-mm diameter capillary connected to the OWR target chamber at a pressure of 300 kPa.